Ion-Surface Interactions 2021 (ISI 2021)
23-27 August, Yaroslavl, Russia

# SPATIAL DISTRIBUTION OF SECONDARY IONS FROM SINGLE CRYSTAL AND AMORPHOUS TARGETS
# ПРОСТРАНСТВЕННОЕ РАСПРЕДЕЛЕНИЕ ВТОРИЧНЫХ ИОНОВ ДЛЯ МОНОКРИСТАЛЛИЧЕСКИХ И АМОРФНЫХ МИШЕНЕЙ

K.A.Tolpin and V.E.Yurasova
*Faculty of Physics Moscow State University*
*e-mail: ktolpin@mail.ru*

Using the coincidence method [1] the spatial distributions of excited secondary ions of certain energy formed during ion bombardment at various angles of the face (111) and amorphized silicon surface are obtained. The plant has three channels for recording secondary particles emitted as a result of ion bombardment: ion, photon and electron (Fig.1). The analysis of secondary particles by energy is carried out using a spherical electrostatic analyzer.

For comparison with the experimental result, a calculation was made using the theory developed in [2].

The obtained results open the prospect for the approached of coincidence technique to investigate electronic properties of surfaces.

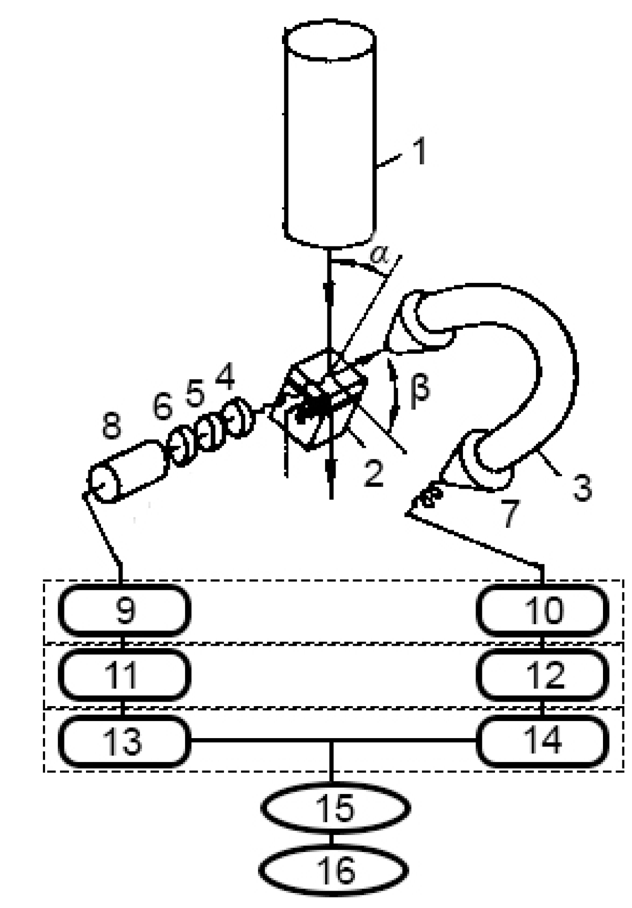


Fig. 1. Block diagram of the apparatus.

## SINGLE CRYSTAL

Distributions on the polar emission angles of the excited $Si^{+*}$ ions produced in the (111) Si face under ion bombardment were measured for two excited states:

**1. $Si^{+*}$ $4p(^2P^0)$ with $E_{exc}$ = 10.07 eV** (see Figure 2)

The distributions exhibit the main maxima at θ = 45° and the local maxima at 35° and 55° which correspond to the preferred yield of sputtered particles in the [011] and [122] close packing directions.

At a secondary $Si^+$ ion energy of 670 eV, the distributions are located nearer to the surface. The calculation distributions of $Si^{+*}$ $4p(^2P^0)$ on the polar emission angles under $Ne^+$ ion bombardment are somewhat narrower than under $Ar^+$ ion bombardment and are more different at secondary ion energies of 150 eV and 670 eV.

**2. $Si^{+*}$ $4p(^4D)$ ($E_{exc}$ = 16.39 eV)** was studied by measuring the number of 567 nm photon coincidences with 300 eV and 600 eV $Si^+$ ions.

The distributions proved to be of the same character as in the previous case and were located nearer to the surface at lower energies of secondary $Si^+$ ions.

At the same time, the difference between the $Si^{+*}$ (567 nm) curves corresponding to the secondary $Si^+$ ion energies of 300 eV and 600 eV proved to be greater compared with the $Si^{+*}$ (386 nm) curves corresponding to 150 eV and 670 eV.

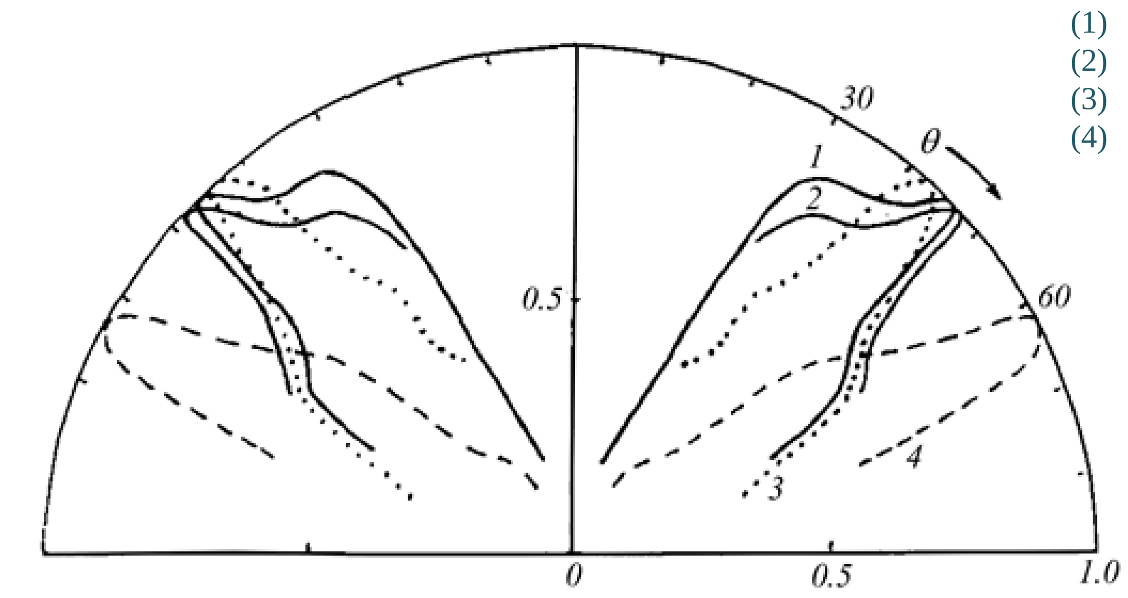


Fig. 2. Polar angle distribution of the intensity $I$ of the emission of $Si^{+*}$ $4p(^2P^0)$ excited secondary ions ($\lambda$ = 386 nm) from the (111) Si face under 8 keV $Ar^+$ and $Ne^+$ ion bombardment at the angle $\alpha$ = 3° to a surface normal in the (110) plane.
The solid curves are experimental data, the dashed and dotted curves are the calculation results for $Si^0$.

## AMORPHOUS

Figure 3 shows the results of studying the secondary $Si^+$ ion distribution on the polar emission angle for amorphous silicon surface under ion bombardment near a surface normal ($\alpha$ = 3°) for secondary $Si^+$ ion energies of 150 eV and 670 eV.

It is seen that, as the $Si^+$ ion energy increases, the distributions get broader and shift towards the surface. In the case of $Ne^+$ ion bombardment, the distributions are located slightly nearer to the surface compared with $Ar^+$ ion bombardment.

The $Si^+$ distributions of polar emission angle $Si^+(\theta)$ are located nearer to the surface than the distributions $Si^{+*}(\theta)$ under the same initial conditions.

The difference between $Si^+(\theta)$ and $Si^{+*}(\theta)$ is greater at the higher energies of secondary ions (670 eV).

The angular distributions of the 300 eV and 600 eV $Si^+$ ions obtained for silicon surface under ion bombardment at $\alpha$ = 35° are located nearer to the surface than at $\alpha$ = 3°.

As in Figure 2, the distribution of the higher-energy $Si^+$ ions is located nearer to the surface. The 4 eV and 18 eV $Si^+$ ion distributions on polar emission angle $\theta$ are located near a surface normal and get broader as the $Si^+$ ion energy increases.

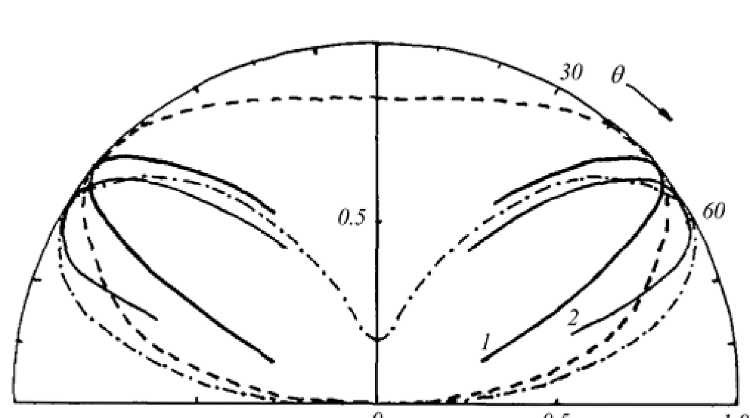


Fig. 3. Polar angle distribution of the intensity $I$ of the emission of $Si^+$ secondary ions from amorphous silicon surface under 8 keV $Ar^+$ ion bombardment at the angle $\alpha$ = 3°.

## Explanations

The observed features of the spatial distributions (Figures 2 and 3) cannot be explained in terms of the conventional sputtering theory.

A more general approach [3] allows for the anisotropy of the collision cascade development and describes the emitted particle distribution.

The anisotropic character of the experimental spatial distributions of secondary ions in their excited and ground states is defined mainly by sputtering features [4, 5].

At the same time, some of the behavioural features, associated with the difference in the spatial distributions of ions in their different excited states, can be analyzed qualitatively.

The kinetic mechanism is the most probable mechanism for production of an excited ion.

The rigid collisions of particles give rise to a hole on the deep *L*-shell which gets filled due to excited ions.

The probability for an excited ion to be produced will be assumed to be independent of particle motion direction and, besides, the spatial distribution of excited ions will be considered as defined by the distribution of all sputtered particles of a given energy $S^0(\theta)$ and by the dependence of the probability for such a state to survive on the emission angle $\theta$.

The probability for an electron to survive at an excited level with subsequent light emission may be described as $P^* \sim \exp(-V_0^*/V_\perp)$, where $V_\perp$ is the perpendicular velocity component with respect to the surface; $V_0^*$ is a parameter describing the rate of the emission less de-excitation processes.

It can readily be verified that the distribution $S^0(\theta)P^*(\theta)$ shifts closer to a normal as the $V_0^*$ value in the $P^*(\theta)$ expression increases. As a rule, the values $V_0^* \sim 10^8$ cm/s are higher than the respective values $V_0^*$ $10^6$-$10^7$ cm/s for the probability of ion production in ground state [4]. Therefore, the spatial $Si^+$ ion distributions are located below the respective distributions of excited particles.

## Conclusions

- At low energies of the analyzed secondary ions (on the order of eV units), the maximum distribution of $I(\theta)$ is located normal to the surface. As the energy of the secondary ions $E_i$ increases, the $I(\theta)$ becomes wider and shifts towards the surface for greater $E_i$. This pattern is observed for secondary ions in both main and excited states.
- The angular distribution of secondary ions in the main state lies closer to the surface than the distribution of excited ions of the same energy. The maximum distribution along the polar angle of emission approaches the surface as the excitation energy of the secondary ion decreases.
- With neon ion bombardment, the distribution of secondary $Si^+$ ions is more knotty than with argon irradiation, and shifted slightly closer to normal to the surface for large $E_i$.
- The difference in the angular distributions of fast secondary $Si^+$ ions with $E_i$ = 150 and 670 eV over the polar yield angle in the case of neon spraying is much larger than in argon irradiation.
- The experimental angular distributions of ions in the main and excited state are in qualitative agreement with the data of the Roosendaal-Sanders sputtering theory [6].

## References

[1] D.Ledyankin, I.Urazgildin, V.Yurasova, J. of Experiment. and Theor. Phys. 94 (1988) 90.
[2] I.Urazgildin and A.Borisov, Vacuum. 40 (1990) 461.
[3] K.A.Tolpin, K.F.Minnebaev, V.E.Yurasova, J. Surf. Invest.: X-ray, Synchr. and Neutr. Tech.14 (2020), 4, 706.
[4] W.F.van der Weg, N.Tolk, C.W.White and Y.M.Kraus, Nucl. Instr. and Meth. 132 (1976) 405.
[5] V.E.Yurasova, N.V.Pleshivtsev, I.V.Orfanov, J. of Experiment. and Theor. Phys. 37 (1960) 689.
[6] H.E.Roosendaal and J.B.Sanders, Rad. Eff. 52 (1980) 137.